

# The AL-Gaussian Distribution as the Descriptive Model for the Internal Proactive Inhibition in the Standard Stop Signal Task

Mohsen Soltanifar<sup>a</sup>, Michael Escobar<sup>b</sup>, Annie Dupuis<sup>c</sup>, Andre Chevrier<sup>d</sup> and Russell Schachar<sup>e</sup>

<sup>a,b,c</sup> Biostatistics Division, Dalla Lana School of Public Health, University of Toronto, Toronto, M5T 3M7, ON, Canada ; <sup>a,c,d,e</sup> Department of Psychiatry, The Hospital for Sick Children, 555 University Avenue, Toronto, M5G 1X8, ON, Canada

## ARTICLE HISTORY

Compiled May 28, 2022

## ABSTRACT

Measurements of response inhibition components of reactive inhibition and proactive inhibition within the stop signal paradigm have been of special interest for researchers since the 1980s. While frequentist nonparametric and Bayesian parametric methods have been proposed to precisely estimate the entire distribution of reactive inhibition, quantified by stop signal reaction times(SSRT), there is no method yet in the stop signal task literature to precisely estimate the entire distribution of proactive inhibition. We introduce an Asymmetric Laplace Gaussian (ALG) model to describe the distribution of proactive inhibition. The proposed method is based on two assumptions of independent trial type(go/stop) reaction times, and Ex-Gaussian (ExG) models for them. Results indicated that the four parametric, ALG model uniquely describes the proactive inhibition distribution and its key shape features; and, its hazard function is monotonically increasing as are its three parametric ExG components. In conclusion, both response inhibition components can be uniquely modelled via variations of the four parametric ALG model described with their associated similar distributional features.

## KEYWORDS

Proactive Inhibition, Reaction Times, Ex-Gaussian, Asymmetric Laplace Gaussian, Bayesian Parametric Approach, Hazard function.

## 1. Introduction

Response inhibition refers to one's ability to stop responses or impulses that just became inappropriate or unwanted within constantly changing environments,[1]. The importance of this process lies in one's being in constantly changing conditions, which require new, updated courses of action,[2]. Some instances of response inhibition in daily life include braking while driving a vehicle into an intersection in reaction to a sudden traffic change, changing direction during a tennis game, and resisting an extra piece of pizza at a birthday party. Two paradigms have been proposed to study the response inhibition in the lab setting, [3]: the stop signal task and the Go/No-go task. In the standard stop signal task, as used in this study, the task consists of a two-choice, response time task called the "go task" and the "stop task". The go task is the primary

task in which the participants are asked to correctly press a right or left button, in response to stimulus presentation, an “X” or “O” on the computer screen . The stop task is the occasional, secondary task in which (with probability of stop signal  $p_{ss}$ ) the participants are presented an stop signal alarm after a temporal delay; Participants are instructed to withhold their responses to the ongoing go task. Successful response inhibition occurs when participants successfully withhold their response to the “X” or “O” on the screen in the stop task (Figure 1).

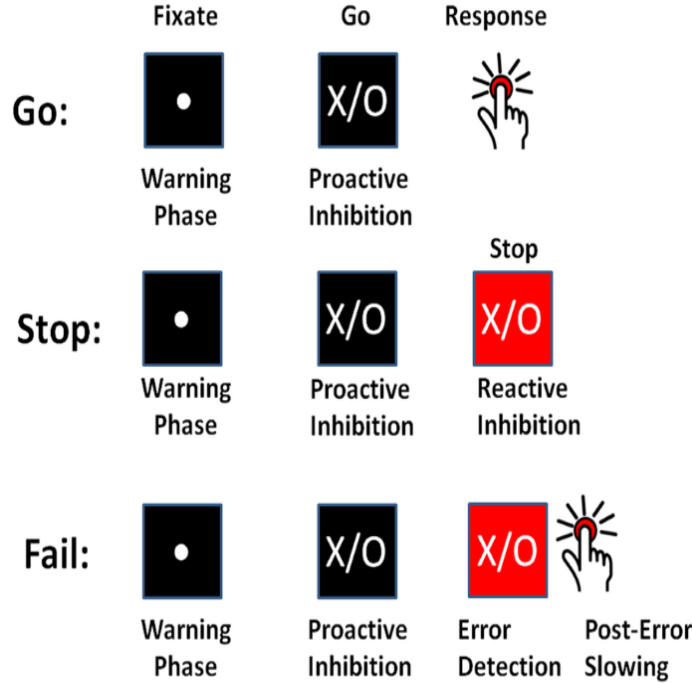


**Figure 1.:** The standard stop signal task with two inhibition components: proactive inhibition, reactive inhibition [4]

Response inhibition has two distinctive temporal-dynamic components: reactive inhibition and the proactive inhibition. Both components have been utilized within the standard stop signal task, or its varieties, to discriminate different clinical groups, [5,6]. We refer to reactive inhibition as the outright inhibition triggered by an external cause, while proactive inhibition is restraint of actions in preparation for stopping by external conditions, [7]. Each of these inhibition components have been quantified in distinctive methods in the stop signal task (SST) literature.

Reactive inhibition has been quantified as Stop Signal Reaction Times (SSRT) in the SST literature from both point estimation and distributional perspectives. Major point estimations of the reactive inhibition up to now include the Crude SSRT, the Logan 1994 SSRT, [1], the Weighted SSRT, the Mixture SSRT, [8], and the time series-based SSRT,[9]. On the other hand, major distributional estimations of the reactive inhibition include the Colonius’s nonparametric method,[10], the Bayesian Parametric Approach (BPA), [11,12] — with two subtype methods: the Individual BPA (IBPA) and the Hierarchical BPA(HBPA) — and the mixture method, [13]. In the mixture method, the entire SST data is partitioned to type A SST data, trials following a go trial, and type B SST data, trials following a stop trial; The trial type weights are defined as  $W_A^c$  =proportion of type A stops within all stops,  $W_B^c = 1 - W_A^c$ . Now, for

$W_A \sim \text{Bernoulli}(W_A^c)$ ,  $W_B \sim \text{Bernoulli}(W_B^c)$ , and fitted cluster type  $SSRT_A$ ,  $SSRT_B$  distributions by the former two methods, the mixture index for the reactive inhibition is defined as:

$$SSRT_{Mixture} = {}^d W_A \times SSRT_A + W_B \times SSRT_B. \quad (1)$$

Note that for the case of parametric mixture SSRT, the cluster type components  $SSRT_A$ , and  $SSRT_B$  may take a variety of proposed reaction time (RT) models, such as Ex-Gaussian (ExG), Ex-Wald, Wald, Gamma, Weibull and lognormal, [14–16]. However, given practical advantages of the ExG model to others, it is widely considered as the parametric model for the reactive inhibition, [11,12].

Proactive inhibition has been quantified in the SST literature merely as point estimation from different perspectives. The first such estimation is defined through a dynamic Bayesian model, [17]. Here, using the mixture assumption for the predictive distribution for the probability of the kth trial being a stop task “ $p(\text{Stop})$ ,” the reactive inhibition is defined as the following positive Pearson correlation:

$$\text{Sequential.Effect} = \text{Corr}(p(\text{Stop}), \text{GORT}). \quad (2)$$

The second estimation is based on the variation of differences of reaction times in a go trial (GORTs) in the associated arms of the modified standard stop signal task paradigm, [18–23]. Generally, for two given probabilities of stop signals in two arms of the modified SST where  $0 \ll p_{ss}^{(1)} < p_{ss}^{(2)} \ll 1$ , it is defined by as:

$$\Delta \text{GORT} = \text{mean}(\text{GORT}_{(p_{ss}^{(2)})}) - \text{mean}(\text{GORT}_{(p_{ss}^{(1)})}). \quad (3)$$

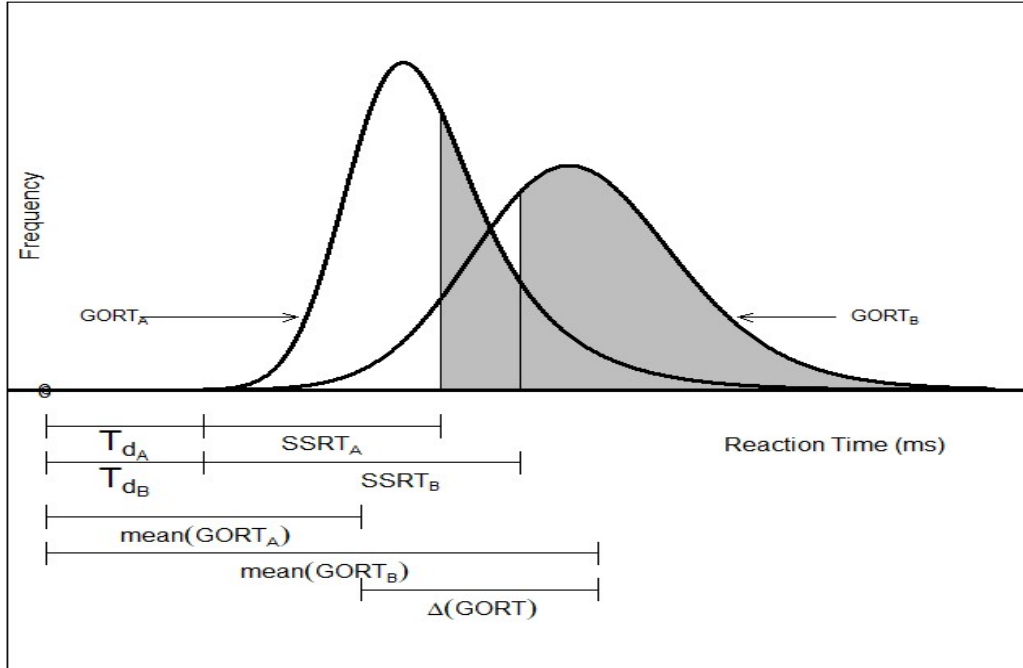


**Figure 2.:** Trial type point estimation of proactive inhibition in the standard stop signal task

The last type of the point estimation of proactive inhibition is based on the differences of GORTs in the trial type clusters of the standard SST paradigm [8,9](Figure.2.). Here, for the fixed stop signal probability (e.g.  $p_{ss} = 0.25$ ) and the type A GORTA and type B GORTB, it is defined as:

$$\Delta GORT = \text{mean}(GORT_B) - \text{mean}(GORT_A). \quad (4)$$

However, little information is available in the SST literature on the entire distribution of proactive inhibition and its key features. This subject is particularly important as measures of central tendency, such as mean or median, are insufficient — and even unnecessary — to compare mostly skewed response inhibition distributions,[24]. In addition, masking prominent features of the proactive inhibitions by using measures of central tendency may result in incorrect conclusions about their make-up. As an example, two different clinical groups may have same mean of proactive inhibition, but the shape of their distributions may differ: one may be more positively skewed, or more leptokurtic, or possess higher domain of variance. The above mentioned methods of estimation of proactive inhibition do not allow for precise estimation and description of the appropriate models for the entire set of proactive inhibition distributions.

This study proposes a four parametric, Asymmetric Laplace Gaussian (ALG) model for the entire proactive inhibition, given the assumption of independent trial type (go/stop) GORTs within the standard stop signal task. The study outline follows. First, as in [8,9] the overall SST data for each participant is partitioned to type A SST data and type B SST data. Second, using the Individual Bayesian Parametric Approach (IBPA) method [11,12], the fitted ExG GORT mean posterior parameters are calculated for the cluster type SST data; then the distribution of proactive response inhibition is introduced as the difference of two independent fitted GORT ExG models, and it is shown that it has a four-parametric ALG distribution. Third, the descriptive statistics, shape statistics, and key distributional properties of the ALG model, such as component decomposition, shape and tail behavior and monotonic hazard function, are discussed. Finally, an empirical example is presented to manifest the above presented results.

## 2. Materials & Methods

### 2.1. Data

The study data have been previously described [8,9,13,25]. Data were collected at the Ontario Science Center in Toronto, Canada in 2009-2010. Included were 16,099 participants aged 6 to 17. The participants' parents provided the required ethical consent for the SST experiment. Each participant completed the SST task including 4 blocks of 24 trials with total of 96 trials, including random 25% stop trials (24 stops) and 75% go trials(72 goes). The SST tracking algorithm was designed so that at the end of trials, each participant achieves a 50% probability of successful inhibition.

### 2.2. Participants

The study participants are the same as those described in [9,13]. Included here is a unique subsample of 44 participants with mean age of 12.1 years, with 96 SST trials for each, and with an almost balanced number of trial type stop trials (10-14 type B stop

trials vs. 14-10 type A stop trials, respectively). This almost balanced number of trial type stop trials yields 30-42 type B go trials vs. 42-30 type A stop trials, respectively.

### 2.3. The SST Clusters

The study Stop Signal Task clusters have been described before in [8,9,13]. Each participant's SST data was partitioned to type A SST data, where all trials were preceded by a go trial, and type B SST data, all trials preceded by a stop trial. Hence, each participant has three types of SST data clusters: Type-A SST cluster (i.e., 56 trials), Type B SST cluster (i.e., 40 trials), and Type-S SST cluster (all 96 trials). Then, using IBPA, the parameters of the corresponding Ex-Gaussian (ExG) GORT's parameters (i.e.  $\theta_A = (\mu_A, \sigma_A, \tau_A)$ ,  $\theta_B = (\mu_B, \sigma_B, \tau_B)$ ,  $\theta_S = (\mu_S, \sigma_S, \tau_S)$ ) were computed as described in the upcoming results section 3.2.

### 2.4. Preliminaries on Component Distributions

The first two definitions provide the key features of the components of our upcoming calculations, namely Ex-Gaussian distribution (ExG), [26], and the Asymmetric Laplace distribution (AL), [27].

**Definition 2.1.** A random variable has an Ex-Gaussian (ExG) distribution with parameters  $(\mu, \sigma, \tau)$  whenever it is considered as the sum of an independent normal random variable with parameters  $(\mu, \sigma^2)$  and an exponential random variable with parameter  $\tau$ :

$$ExG(\mu, \sigma, \tau) \stackrel{d}{=} N(\mu, \sigma^2) \oplus Exp(\tau). \quad (5)$$

The density, the moment generating function, the  $n$ th cumulant ( $n \geq 1$ ), the variance, the skewness and the kurtosis of the ExG distribution are given by:

$$\begin{aligned} PDF & f_{ExG}(t|\mu, \sigma, \tau) = \frac{1}{\tau} \exp\left(\frac{\mu - t}{\tau} + \frac{\sigma^2}{2\tau^2}\right) * \Phi\left(\frac{\mu - t}{\sigma} - \frac{\sigma}{\tau}\right) : \sigma, \tau > 0, t \in \mathbb{R}, \\ MGF & m_{ExG}(t) = (1 - t\tau)^{-1} \exp\left(\mu \cdot t + \frac{\sigma^2}{2} t^2\right) : t < \tau^{-1}, \\ n^{th} Cumulant & \kappa_n^{ExG} = (n - 1)! \tau^n + 1_{n=1}(n)\mu + 1_{n=2}(n)\sigma^2 : 1 \leq n, \\ Mean & E(ExG) = \mu + \tau, \\ Variance & Var(ExG) = \sigma^2 + \tau^2, \\ Skewness & \gamma_{ExG} = 2(1 + \sigma^2\tau^{-2})^{-3/2}, \\ Kurtosis & \kappa_{ExG} = 3 \frac{(1 + 2\sigma^{-2}\tau^2 + 3\sigma^{-4}\tau^4)}{(1 + \sigma^{-2}\tau^2)^2}. \end{aligned} \quad (6)$$

**Definition 2.2.** A random variable has an Asymmetric Laplace (AL) distribution with parameters  $(\alpha_1, \alpha_2)$  whenever it is considered as the difference of two independent exponential random variables with parameters  $\alpha_2$ , and  $\alpha_1$ , respectively:

$$AL(\alpha_1, \alpha_2) \stackrel{d}{=} Exp(\alpha_2) \ominus Exp(\alpha_1). \quad (7)$$

The density, the moment generating function, the  $n$ th cumulant ( $n \geq 1$ ), the variance, the skewness and the kurtosis of the AL distribution are given by:

$$\begin{aligned}
\text{PDF} & f_{AL}(t|\alpha_1, \alpha_2) = \frac{\exp(\frac{t}{\alpha_1})1_{(-\infty,0)}(t) + \exp(\frac{-t}{\alpha_2})1_{[0,\infty)}(t)}{\alpha_1 + \alpha_2} \quad t \in \mathbb{R}, \\
\text{MGF} & m_{AL}(t) = (1 + (\alpha_1 - \alpha_2)t - \alpha_1\alpha_2.t^2)^{-1} \quad -\alpha_1^{-1} < t < \alpha_2^{-1}, \\
n^{\text{th}}\text{Cumulant} & \kappa_n^{AL} = (n-1)!((-\alpha_1)^n + (\alpha_2)^n) \quad 1 \leq n, \\
\text{Mean} & E(AL) = -(\alpha_1 - \alpha_2), \\
\text{Variance} & \text{Var}(AL) = \alpha_1^2 + \alpha_2^2, \\
\text{Skewness} & \gamma_{AL} = -2(\alpha_1^3 - \alpha_2^3) \times (\alpha_1^2 + \alpha_2^2)^{-3/2}, \\
\text{Kurtosis} & \kappa_{AL} = 3(3\alpha_1^4 + 2\alpha_1^2\alpha_2^2 + 3\alpha_2^4) \times (\alpha_1^2 + \alpha_2^2)^{-2}. \tag{8}
\end{aligned}$$

The convolution of two independent, AL random variables and Gaussian random variables, called ALG or Normal-Laplace (NL) random variables, has been of special attention in the literature [28,29].

**Definition 2.3.** A random variable has Asymmetric Laplace-Gaussian (ALG) distribution with parameters  $(\alpha_1, \alpha_2, \mu, \sigma)$  whenever it is considered as the sum of two independent, Asymmetric Laplace random variables with parameters  $(\alpha_1, \alpha_2)$ , and a Normal random variable with parameters  $(\mu, \sigma^2)$ , respectively:

$$ALG(\alpha_1, \alpha_2, \mu, \sigma) \stackrel{d}{=} AL(\alpha_1, \alpha_2) \oplus N(\mu, \sigma^2). \tag{9}$$

Note that since  $AL(0^+, \alpha_2) \stackrel{d}{=} Exp(\alpha_2)$ , it follows that  $ALG(0^+, \alpha_2, \mu, \sigma) \stackrel{d}{=} ExG(\mu, \sigma, \alpha_2)$ . Consequently, the ExG model can be considered a special degenerate ALG model. Next, the following key Theorems equip us to propose the ALG distribution as the model for the proactive inhibition and compute the key descriptive and shape statistics of the ALG distribution in terms of its Laplacian and Gaussian components,[30].

**Theorem 2.4.** Let  $X, Y$  be two independent, real-valued random variables with finite, moment generating function  $m_X, m_Y$ , and cumulant functions  $\kappa, \kappa$ , respectively. Then, for some  $s_0 > 0$  :

$$m_{X+Y}(t) = m_X(t)m_Y(t) : \quad (-s_0 < t < s_0), \tag{10}$$

$$\kappa_{X+Y}(t) = \kappa_X(t) + \kappa_Y(t) : \quad (-s_0 < t < s_0). \tag{11}$$

**Theorem 2.5.** Let  $X, Y$  be two real-valued random variables with finite moment generating functions  $m_X, m_Y$ , respectively. Assume for some  $s_0 > 0$  :  $m_X(t) = m_Y(t)$   $(-s_0 < t < s_0)$ . Then,  $X, Y$  have the same distribution.

Finally, the last two theorems enable us to describe the behavior of the hazard function of the ALG model for the proactive inhibition, [31].

**Theorem 2.6.** Let  $X$  be a real-valued random variable with differentiable PDF  $f_X$  and CDF  $F_X$  such that  $f_X(t) \rightarrow 0, F_X(t) \rightarrow 1$  as  $t \rightarrow \infty$ , and  $-\ln(f_X(t))$  is convex(concave). Then, the hazard function  $h_X$  is increasing(decreasing).

**Theorem 2.7.** Let  $X, Y$  be two independent, real-valued random variables with (strictly) increasing hazard functions  $h_X, h_Y$ , respectively. Then, the hazard function of their sum,  $h_{X+Y}$  is (strictly) increasing as well.

## 2.5. Proactive Inhibition Index

Proactive inhibition was operationalized based on the internal perspective in the standard stop signal task,[9]. Here, for a given fixed stop signal probability (e.g. 0.25), type A GORT of  $GORT_A$  (GORT for a trial after a go trial), and type B GORT of  $GORT_B$  (GORT for a trial after a stop trial), the internal proactive inhibition is defined as:

$$\Delta GORT =^d GORT_B - GORT_A. \quad (12)$$

Note that there are two mathematical perspectives for the proactive inhibition: First, a model with two ExG components; Second, a model with Asymmetric Laplace (AL) and Gaussian components. Henceforward, it is understood within the given context which perspective is being discussed.

## 2.6. Statistical Analysis

The statistical ALG model to describe the proactive inhibition distribution was presented using the method of moment generating functions, [29]. Next, the descriptive and shape statistics of the ALG model were computed in terms of parameters of the cluster type ExG components,[30]. Finally, its hazard function behavior was theoretically inferred using its components' parameters [31].

The ExG components of the presented statistical model were estimated using the IBPA method,[11,12]. As in [13], each participant had three IBPA associated ExG parametric estimations  $\theta_A = (\mu_A, \sigma_A, \tau_A)$ ,  $\theta_B = (\mu_B, \sigma_B, \tau_B)$ , and  $\theta_S = (\mu_S, \sigma_S, \tau_S)$ , associated to type-A cluster SST data, type-B cluster SST data, and the entire SST data, respectively. These parameters were estimated as the posterior means of the associated following IBPA procedure with 3 chains, 5,000 burn ins within 20,000 simulations in Bayesian Ex-Gaussian Estimation of Stop-Signal RT distributions (BEESTS) 2.0 software,[12]:

Data	Individual Priors
$GORT \sim ExG(\mu_{go}, \sigma_{go}, \tau_{go})$	
$SRRT \sim ExG(\mu_{go}, \sigma_{go}, \tau_{go}, \mu_{stop}, \sigma_{stop}, \tau_{stop}, SSD)I_{[1,1000]}^+$	$\mu_{go}, \sigma_{go}, \tau_{go} \sim U[10, 2000]$
$SSRT \sim ExG(\mu_{go}, \sigma_{go}, \tau_{go}, \mu_{stop}, \sigma_{stop}, \tau_{stop}, SSD)I_{[1,1000]}^+$	$\mu_{go}, \sigma_{go}, \tau_{go} \sim U[10, 2000]$

Two sets of comparisons were conducted using paired t-tests (DescTools, R software version 4.0.0, [32]): First, a primary comparison between cluster-type fitted parameter of the ExG distribution, the descriptive statistics, and the shape statistics; second, secondary comparisons between the ALG model descriptive and shape statistics and its associated cluster-type ExG components.

## 3. Results

The results are divided into two subsections. In subsection 3.1, we explore the mathematical analysis of the proposed model for the proactive inhibition in the standard stop signal task. This includes a four parametric, ALG for the proactive inhibition and its prominent distributional properties. In subsection 3.2, we present an empirical example of the case and discuss its various distributional features.

### 3.1. Mathematical Analysis

#### 3.1.1. The Proactive Inhibition Distribution and its Parameters

First of all, we propose a mathematical model for the proactive inhibition provided by the ALG:

**Theorem 3.1. (The Main Result).** *The four parametric ALG( $\tau_A, \tau_B, \mu_B - \mu_A, (\sigma_B^2 + \sigma_A^2)^{1/2}$ ) presents a model for the Internal Proactive Inhibition Index  $\Delta GORT$  with trial type-related parameters ( $\mu_A, \sigma_A, \tau_A, \mu_B, \sigma_B, \tau_B$ ) in the Standard Stop Signal Task.*

As a corollary of Theorem 3.1, the probability density function ( $f_{\Delta GORT}$ ) and the cumulative density function ( $F_{\Delta GORT}$ ) of the ALG distribution for the Internal Proactive Inhibition Index are given by [28,29],:

$$\begin{aligned}
 f_{\Delta GORT}(t) &= \frac{1}{\tau_A + \tau_B} \\
 &\times \left[ e^{\left(\frac{\sqrt{\sigma_B^2 + \sigma_A^2}}{2\tau_B}\right)\left(\frac{\sqrt{\sigma_B^2 + \sigma_A^2}}{\tau_B} - 2\frac{t - (\mu_B - \mu_A)}{\sqrt{\sigma_B^2 + \sigma_A^2}}\right)} \times \left(1 - \Phi\left(\frac{\sqrt{\sigma_B^2 + \sigma_A^2}}{\tau_B} - \frac{t - (\mu_B - \mu_A)}{\sqrt{\sigma_B^2 + \sigma_A^2}}\right)\right) \right. \\
 &+ \left. e^{\left(\frac{\sqrt{\sigma_B^2 + \sigma_A^2}}{2\tau_A}\right)\left(\frac{\sqrt{\sigma_B^2 + \sigma_A^2}}{\tau_A} + 2\frac{t - (\mu_B - \mu_A)}{\sqrt{\sigma_B^2 + \sigma_A^2}}\right)} \times \left(1 - \Phi\left(\frac{\sqrt{\sigma_B^2 + \sigma_A^2}}{\tau_A} + \frac{t - (\mu_B - \mu_A)}{\sqrt{\sigma_B^2 + \sigma_A^2}}\right)\right) \right] \\
 & \qquad \qquad \qquad t \in \mathbb{R} \qquad (13)
 \end{aligned}$$

and

$$\begin{aligned}
 F_{\Delta GORT}(t) &= \frac{1}{\tau_A^{-1} + \tau_B^{-1}} \times [(\tau_A^{-1} + \tau_B^{-1})\Phi\left(\frac{t - (\mu_B - \mu_A)}{\sqrt{\sigma_B^2 + \sigma_A^2}}\right) \\
 &- \tau_A^{-1} e^{\left(\frac{\sqrt{\sigma_B^2 + \sigma_A^2}}{2\tau_B}\right)\left(\frac{\sqrt{\sigma_B^2 + \sigma_A^2}}{\tau_B} - 2\frac{t - (\mu_B - \mu_A)}{\sqrt{\sigma_B^2 + \sigma_A^2}}\right)} \times \left(1 - \Phi\left(\frac{\sqrt{\sigma_B^2 + \sigma_A^2}}{\tau_B} - \frac{t - (\mu_B - \mu_A)}{\sqrt{\sigma_B^2 + \sigma_A^2}}\right)\right) \\
 &+ \tau_B^{-1} e^{\left(\frac{\sqrt{\sigma_B^2 + \sigma_A^2}}{2\tau_A}\right)\left(\frac{\sqrt{\sigma_B^2 + \sigma_A^2}}{\tau_A} + 2\frac{t - (\mu_B - \mu_A)}{\sqrt{\sigma_B^2 + \sigma_A^2}}\right)} \times \left(1 - \Phi\left(\frac{\sqrt{\sigma_B^2 + \sigma_A^2}}{\tau_A} + \frac{t - (\mu_B - \mu_A)}{\sqrt{\sigma_B^2 + \sigma_A^2}}\right)\right)] \\
 & \qquad \qquad \qquad t \in \mathbb{R}, \qquad (14)
 \end{aligned}$$

respectively. Here  $\Phi$  denotes the standard normal cumulative distribution function.

Next, given trial type parameters, we estimate the descriptive and shape statistics for the proposed ALG model of the proactive inhibition:

**Theorem 3.2.** *The descriptive statistics and the shape statistics of the Proactive Inhibition ALG distribution with trial type-related parameters ( $\mu_A, \sigma_A, \tau_A, \mu_B, \sigma_B, \tau_B$ ) in the standard stop signal task are given by:*



$$\begin{aligned}
n^{\text{th}} \text{Cumulant} \quad \kappa_n^{\text{ALG}} &= (n-1)!((- \tau_A)^n + \tau_B^n) \\
&\quad + 1_{(n=1)}(n)(\mu_B - \mu_A) + 1_{(n=2)}(n)(\sigma_B^2 + \sigma_A^2) : \quad 1 \leq n \\
\text{Mean} \quad E(\text{ALG}) &= \tau_B - \tau_A + \mu_B - \mu_A, \\
\text{Variance} \quad \text{Var}(\text{ALG}) &= \tau_A^2 + \tau_B^2 + \sigma_A^2 + \sigma_B^2, \\
\text{Skewness} \quad \gamma_{\text{ALG}} &= \frac{2(\tau_B^3 - \tau_A^3)}{(\tau_A^2 + \tau_B^2 + \sigma_A^2 + \sigma_B^2)^{3/2}}, \\
\text{Kurtosis} \quad \kappa_{\text{ALG}} &= \frac{6(\tau_B^4 + \tau_A^4)}{(\tau_A^2 + \tau_B^2 + \sigma_A^2 + \sigma_B^2)^2}. \tag{15}
\end{aligned}$$

### 3.1.2. The Proactive Inhibition's Key ALG Distributional Properties

In this section, we present key distributional properties for the ALG model for proactive inhibition including: (i) component decompositions in terms of trial type GORT; (ii) shape and tail behavior; and, (iii) behavior of the hazard function.

**Theorem 3.3. (Component Decomposition).** *An ALG model for proactive inhibition emerges from uncountable pairs of trial type related GORT ( $GORT_A, GORT_B$ ) distributions.*

We remind the reader that Theorem3.3 presents a process to simulate a plausible four parametric ALG distribution for the proactive inhibition.

**Theorem 3.4. (Shape and Tail Behavior).** *An ALG model for proactive inhibition has unimodal, generally asymmetric, infinite, differentiable density with extreme large values proportionate to the  $\text{Exp}(1/\tau_B)$  distribution.*

We remind the reader that contrary to the mean of the ALG model for proactive inhibition, there are no closed form formulas for the mode and the median, respectively. Similar to ExG model for reactive inhibition with increasing hazard function, we have:

**Theorem 3.5. (Hazard Function's Behavior).** *An ALG model for proactive inhibition has increasing hazard function.*

## 3.2. The Empirical Example

This section presents an example of the empirical data for the theoretical results inferred in the previous section on the ALG model for proactive inhibition and its descriptive, shape and hazard function's key features. These results are based on the cluster type IBPA estimation of mean posterior ExG parameters  $\theta = (\mu, \sigma, \tau)$  presented in TableB1(Appendix B).

The ExG model for each of the two components of proactive inhibition has the following key features presented by the Table 1. First, while type B  $\mu$ , and  $\sigma$  parameters are significantly larger than their type A counterparts, there is no difference for the  $\tau$  parameter. In addition, the sample average proactive inhibition is 92.1 ms (95% CI = (69.4,114.9)). Second, both ExG components are positively skewed and leptokurtic. Finally, there is no significance difference between their trial type skewness and their trial type kurtosis, respectively. Figure3a presents the trial type ExG modelled components of the ALG model.

**Table 1.:** Descriptive and paired t-test [mean (95%CI)] results for parameters, descriptive and shape statistics of fitted Ex-Gaussian distribution to cluster type GORT and AL-Gaussian distribution to  $\Delta GORT$ , ( $n = 44$ ).

		ExG model			ALG model
		Cluster	Comparison		Cluster
		Type A	Type B	Type B vs. Type A	Type S
Parameter	$\alpha_1$	-	-	-	104.2
		-	-	-	(90.4,117.9)
	$\alpha_2$	-	-	-	142.4
		-	-	-	(125.9,158.8)
	$\mu$	478.8	532.8	53.9***	53.9
		(448.0,509.7)	(498.6,566.9)	(30.9,76.9)	(30.9,76.9)
	$\sigma$	109.9	133.1	23.2	179.2
	(90.5,129.3)	(108.4,157.8)	(-0.1,46.4)	(151.4,206.9)	
	$\tau$	104.2	142.4	38.2***	-
		(90.4,117.9)	(125.9,158.8)	(19.6,56.8)	-
Statistics	Mean	583.0	675.1	92.1***	92.1
		(553.0,612.9)	(633.8,716.4)	(69.4,114.9)	(69.4,114.9)
	St.D	160.6	202.4	41.8***	260.4
		(143.5,177.8)	(177.9,226.9)	(25.9,57.6)	(232.3,288.6)
	Skewness	0.787	0.918	0.131	0.186
		(0.602,0.973)	(0.751,1.085)	(-0.113,0.375)	(0.076,0.296)
	Kurtosis	4.966	5.300	0.334	1.153
		(4.414,5.518)	(4.790,5.808)	(-0.397,1.064)	(0.923,1.384)

Notes: \*p-value < 0.05; \*\*p-value < 0.005; \*\*\*p-value < 0.0005.

The ALG model for proactive inhibition has the following features, given cluster type parameter estimations. First, as a primary corollary of Theorem 3.2, the model is positively skewed whenever  $\tau_B > \tau_A$ . The negatively skewed and symmetric cases hold whenever the strict greater inequality  $>$  is replaced with  $<$  and  $=$ , respectively. According to appendix TableB1 data, all three cases exist (case 10: positive skew; case 16: symmetric; case 11: negative skew). Figure 3b presents all the mentioned three cases. In overall, the model is positively skewed given results in Table 1. Second, as the secondary corollary of Theorem 3.2, the model is leptokurtic whenever  $(2(\tau_A^4 + \tau_B^4))^{1/2} - (\tau_A^2 + \tau_B^2) > \sigma_A^2 + \sigma_B^2$ . The platykurtic and mesokurtic cases hold whenever the strict greater inequality  $>$  is replaced with  $<$  and  $=$ , respectively. In particular, for the case  $\tau_A \approx \tau_B$ , the model is always platykurtic. In overall, the model is platykurtic given results in Table 1. Third, while the ALG model's standard deviation is larger than its two ExG's components, its skewness and kurtosis are significantly smaller. Finally, the ALG model has strictly increasing hazard function for various cases of skewness as mentioned in Theorem3.5 and presented in Figure 3c.

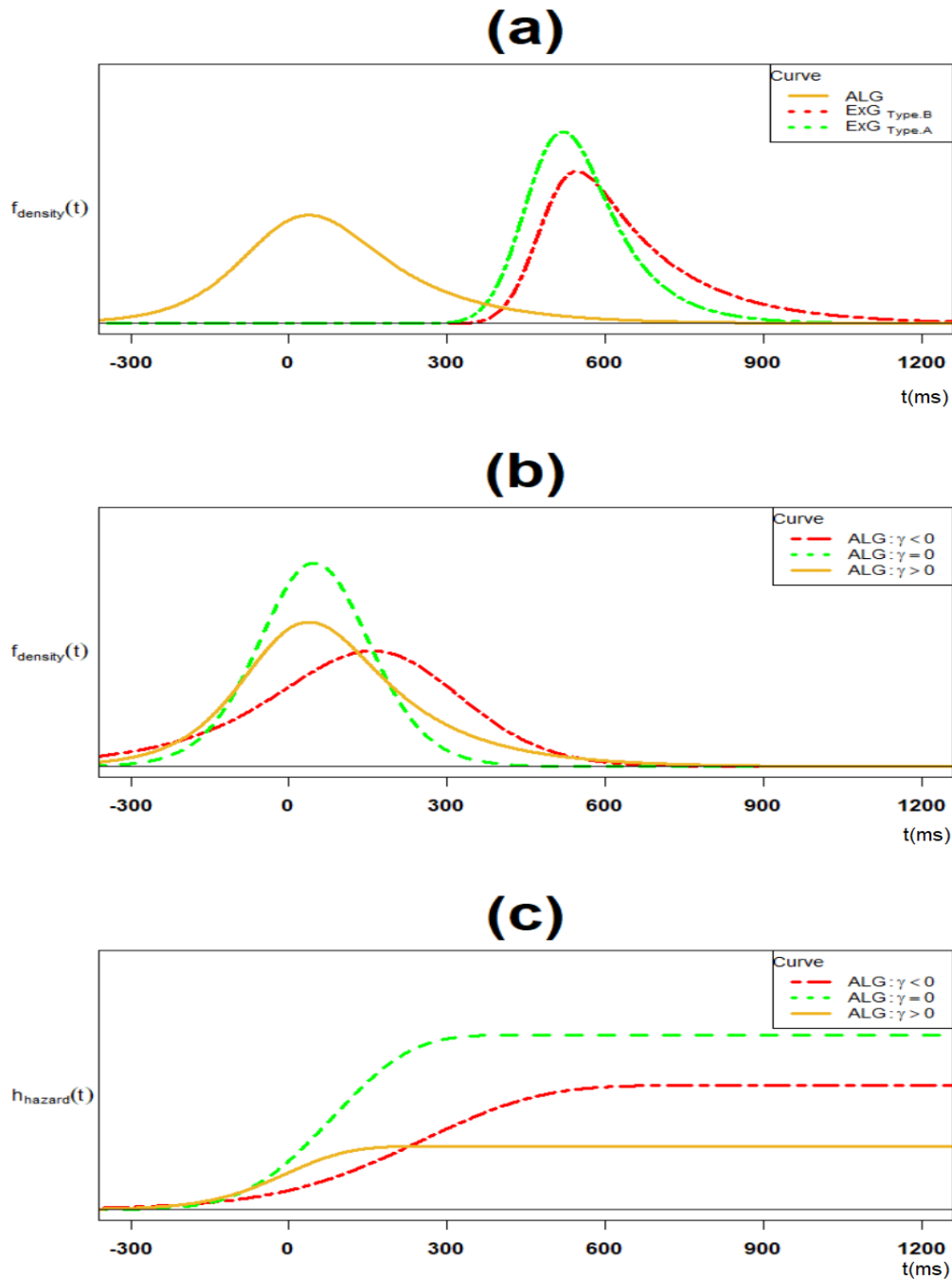


**Figure 3.:** The ALG density and its trial type ExG component densities; (b) The ALG density for the positively skewed, symmetric and negatively skewed cases; (c) The ALG hazard function for the positively skewed, symmetric and negatively skewed cases.

## 4. Discussion

This paper presents a four parametric model for the entire proactive inhibition distribution, the ALG model. This model is based on the two independent ExG components fitted to the trial type GORTs. Considering ExG models as degenerate ALG model, this work indicates that both components of the response inhibition can be modelled by a four parametric ALG model.

The proposed ALG model for the proactive inhibition has several important aspects. First, the model is based on the independent assumption of GORTA and GORTB. Such speculation is warranted by the independent assignment of go trials and stop trials in the entire stop-signal task trials. Hence, via conditioning, their following associated type A go trial and type B go trials are independent, and so are their associated GORTs (i.e., GORTA and GORTB). Second, contrary to the point estimations of proactive inhibition in the form of mean [9] or correlation [17], it presents the entire distribution of the proactive inhibition. Third, contrary to the positively skewed, leptokurtic ExG model for reactive inhibition, the ALG model for proactive inhibition can be negatively skewed, platykurtic. Fourth, similar to the ExG model for reactive inhibition, the ALG model for proactive inhibition has monotonically increasing hazard function. Finally, the ALG model for proactive inhibition with its associated ExG modelled components is unique in the sense that other non-ExG RT models for its components (e.g. Gamma, Weibull, Lognormal, Wald, and Ex-Wald) do not yield to any known closed form distribution for proactive inhibition. This is easily verifiable by repeating the proof of Theorem 3.1 based on uniqueness of moment generating functions for other non-ExG RT models for the trial type GORTs.

The proposed ALG model for the proactive inhibition is estimated (or simulated) in two different methods. First, one may use the Bayesian or frequentist-based methods to fit the ExG parametric models to its trial type components, and then estimate the four parametric ALG model using Theorem 3.1, as done in Section 3.2. Second, one may subtract the trial type GORTs and fit the ALG model directly to the differenced GORT data using Maximum Likelihood (ML) or Expectation Maximization (EM) algorithms [33].

There are some limitations in the proposed ALG model for proactive inhibition. First, since GORTA data and GORTB data are unmatched, there is no way to calculate their correlation quantitatively. Hence, from a quantitative perspective, checking the validity of the assumption of independent GORTA and GORTB is difficult. Second, by its definition, proactive inhibition takes only non-negative values while the presented ALG model takes negative values as well. Third, similar to the ExG model for the reactive inhibition, the ALG model for the proactive inhibition has monotonically increasing hazard function preventing it from being the best fitting model for the cases of proactive inhibition with peaked hazards. Finally, given the calculations' structure of the parameters of ALG model, based on those of ExG components, its parameters' cognitive interpretations are highly dependent on its ExG components inheriting their constraints.

Future research should replicate the proposed approach in modelling the proactive inhibition distribution in this study in other different directions. This further work may include the following perspectives: First, one model should consider peaked hazard functions for the ALG model components to address RT data with such features. Second, there is a need to interpret the proposed ALG distribution parameters in terms of inhibition mechanisms in the brain and vice versa. Third, there is a lack of investigation comparing the proactive inhibition distribution in terms of the usual stochastic

order, the descriptive and shape statistics across a spectrum of clinical groups such as ADHD, OCD, schizophrenia, and drug users. Finally, similar investigations on comparing the proactive inhibition distribution and its above key statistics are plausible in terms of the participants' age.

In conclusion, the ALG model provides a practical description of the proactive inhibition distribution that takes full advantage of its ExG components fitted for the trial type GORTs. It also offers a straightforward, computational analogue of the proactive inhibition, comparable to the ExG model for reactive inhibition. Given the advantages of the estimation of the entire distribution of proactive inhibition over former point estimations, the researchers recommend considering the ALG model as the latest optimal choice to describe the distribution of proactive inhibition.

**Author Contributions:** The authors contributed to the study in the following manner: Conceptualization, M.S.; methodology, M.S.; formal analysis, M.S.; validation, M.E, M.S., A.D and R.S.; investigation, M.E., M.S., A.D and R.S.; data curation, R.S.; writing—original draft preparation, M.S.; writing—review and editing, M.S.,M.E., A.D., A.C., and R.S.; All authors have read and agreed to the submitted version of the manuscript.

### **Disclosure Statement**

Mohsen Soltanifar, Michael Escobar, Annie Dupuis and Andre Chevrier have no financial interests to disclose. Russell Schachar has equity in ehave and has been the on the Scientific Advisory Board(SAB) in Lilly and Highland Therapeutic Inc, Toronto, Canada.

### **Funding**

This work has no external funding.

### **ORCID**

Mohsen Soltanifar: <https://orcid.org/0000-0002-5989-0082>  
Michael Escobar: <https://orcid.org/0000-0001-9055-4709>  
Annie Dupuis: <https://orcid.org/0000-0002-8704-078X>  
Andre Chevrier: <https://orcid.org/0000-0002-4298-9529>  
Russell Schachar: <https://orcid.org/0000-0002-2015-4395>

## Abbreviations

ADHD	Attention Deficit Hyperactivity Disorder
AL	Asymmetric Laplace distribution
ALG	Asymmetric Laplace Gaussian distribution
BEESTS	Bayesian Ex-Gaussian Estimation of Stop Signal RT distributions
BPA	Bayesian Parametric Approach
CDF	Cumulative Density Function
EM	Expectation Maximization
ExG	Ex-Gaussian distribution
GORT	Reaction Time in a go trial
GORTA	Reaction Time in a type A go trial
GORTB	Reaction Time in a type B go trial
HBPA	Hierarchical Bayesian Parametric Approach
IBPA	Individual Bayesian Parametric Approach
MGF	Moment Generating Function
ML	Maximum Likelihood
NL	Normal-Laplace distribution
OCD	Obsessive Compulsive Disorder
PDF	Probability Density Function
SSD	Stop Signal Delay
SRRT	Reaction Times in a failed stop trial
SSRT	Stop Signal Reaction Times in a stop trial
SSRTA	Stop Signal Reaction Times in a type A stop trial
SSRTB	Stop Signal Reaction Times in a type B stop trial
SST	Stop Signal Task
$=^d$	Equality in distribution
$\oplus$	Sum of independent random variables
$\ominus$	Difference of independent random variables

## References

- [1] Matzke, D.; Verbruggen, F.; & Logan G.D. (2018). The Stop Signal Paradigm. In *Steven Handbook of Experimental Psychology and Cognitive Neuroscience* (4th ed). Vol 5. Methodology. John Wiley & Sons. Inc.
- [2] Aron, A. R. (2011). From reactive to proactive and selective control: Developing a richer model for stopping inappropriate responses. *Biological Psychiatry*, 69(12). e55-e68.
- [3] Johnston S, Dinoske A, Smith J, Bang R.J, et al. (2007). The Development of Stop Signal and Go/No-go Response Inhibition in Children Aged 7-12 years: Performance and Event Related Potential Indices . *International Journal of Psychology*, 63: 25-38.
- [4] Chevrier, A., Schachar, R.J. (2020). BOLD differences normally attributed to inhibitory control predict symptoms, not task-directed inhibitory control in ADHD. *Journal of Neurodevelopmental Disorders* 12(8) . <https://doi.org/10.1186/s11689-020-09311-8>
- [5] Zandbelt, B.B. ; Van Buuren M.; Kahn, R.S; & Vink, M. (2011). Reduced Proactive Inhibition in Schizophrenia is related to Corticostriatal dysfunction and poor working memory. *Biological Psychiatry*. 70(12), 1151-1158.
- [6] Van Rooji, S.J.H; Rademaker, A.R.; Kennis, M; Vink, M; Kahn, R.S.; & Geuze, E. (2014). Impaired right inferior frontal gyrus-response to contextual cues in male veterans with PTSD during response inhibition. *Journal of Psychiatry and Neuroscience*. 39(5), 330-338.
- [7] Vink, M; Zandbelt, B.B.; Gladwin, T; Hillegers, M; Hoogendam, JM; Van der Wildenberg,

- WPM; et al. (2014). Frontostriatal Activity and Connectivity Increase During Proactive Inhibition Across Adolescence and Early Adulthood. *Human Brain Mapping*, 35, 4415-4427.
- [8] Soltanifar, M.; Dupuis, A; Schachar, R.;& Escobar, M. (2019).A frequentist mixture modelling of stop signal reaction times. *Biostatistics and Epidemiology*, 3, 90-108.
- [9] Soltanifar, M.; Knight, K.; Dupuis, A.; Schachar, R & Escobar, M. (2020). A Time Series-Based Point Estimation of Stop Signal Reaction Times: More Evidence on the Role of Reactive Inhibition-Proactive Inhibition Interplay on the SSRT Estimations. *Brain Science* , 10, 598.
- [10] Colonius, H.(1990). A. Note on the Stop Signal Paradigm, or How to Observe the Unobservable. *Psychological Review*, 97, 309-312.
- [11] Matzke D, Dolan C.V, Logan G.D, Brown S.D, and et al. (2013). Bayesian Parametric Estimation of Stop Signal Reaction Time Distributions. *Journal of Experimental Psychology: General*, 142(4): 1047-1073.
- [12] Matzke D, Love J, Wiecki T.V, Brown S.D, and et al.(2013). Release the BEESTS: Bayesian Estimation of Ex-Gaussian Stop Signal Reaction Time Distributions. *Frontiers in Psychology*, 4: Article 918.
- [13] Soltanifar, M.; Escobar, M.; Dupuis, A.& Schachar, R. (2021). A Bayesian Mixture Modelling of Stop Signal Reaction Time Distributions. *arXiv: 2010.12705.v2[stat.ME]*.
- [14] Schwarz W. (2001). The Ex-Wald Distribution as a Descriptive Model of Reaction Time Data. *Behavioural Research Methods, Instruments and Computers*, 33(4). 457-469.
- [15] Prado Martine M.d., & Fermin Dr. (2008). A Theory of Reaction Times Distributions, (unpublished). Retrieved on December 15, 2020 (<http://cgprints.org/6310>).
- [16] Rouder J.N. (2005). Are Un-shifted Distributional Models Appropriate for Response Times ? *Psychometrika*, 70, 377-381.
- [17] Ide, J.S.; Shenoy, P. ; Yu, A.J.;& Li, C.S. (2013). Bayesian Prediction and Evaluation in the Anterior Cingulate Cortex. *The Journal of Neuroscience*, 33, 2039-2047.
- [18] Bartholly, S; Rennalls, S.J; Jacques, C; Darby, H; Campbell, IC; Schmidt U; & ODaly, OG. (2017). Proactive and reactive inhibitory control in eating disorders . *Psychiatry Research*, 255, 432-440.
- [19] Castro-Meneses, LJ; Johnston, BW;& Sowman, DF. (2018). The effects of impulsivity and proactive inhibition on reactive inhibition and go process: Insights from vocal and manual stop signal tasks. *Frontiers in Human Neuroscience*, 9, 529.
- [20] Brevers, D; Voubuissou, E.; Dejonghe, F; Dutrieux, J; Detiea, M; Cheron, G; Verbanck, D; & Foucart, J. (2018). Proactive and Reactive Motor Inhibition in Top Athletes versus Nonathletes. *Perceptual Motor Skills*, 125, 289-312.
- [21] Zandbelt, B.B; Bloemendaal, M; Neggers, S.F.W; Kahn, R.S;& Vink, M. (2013). Expectations and Variations: Declining the Neural Network of Proactive Inhibitory Control. *Human Brain Mapping*, 34, 2015-2024.
- [22] Dicaprio, V; Modugno, N; Mancini, C; Olivia, E;& Mirabella, G. (2020). Early Stage Parkinson's Patients Show Selective Impairment in Reactive but not Proactive Inhibition. *Moving Disorders*, 35, 409-418.
- [23] Ramautar, JR; Kok, A;& Riedelinkhof, KR. (2004). Effects of Stop Signal Probability in the Stop Signal Paradigm: The N2/P3 Complex further validated. *Brain Cognition* , 56, 234-252.
- [24] Rousselet, GA;& Wilcox, RR. (2020). Reaction Times and Other Skewed Distributions: Problems with the Mean and Median. *Meta Psychology*, 4, MP 2019.1630.
- [25] Crosbie, J.; Arnold, P.; Peterson, A.D.; Swanson, J., Dupuis, A.; Li, X.; Shan, J.; Goodale, T.; Tam, C.; Strug, L.J.; et al. (2013). Response Inhibition and ADHD Traits: Correlates and heritability in a Community Sample. *Journal of Abnormal Child Psychology*, 41, 497-597.
- [26] Heathcote A. (1996). RTSYS: A DOS Application for the Analysis of Reaction Times Data. *Behavior Research Methods, Instruments and Computers*, 28(3), 427-445.
- [27] Kotz, S; Kozubowski, T.J;& Podgorski, K. (2001). *The Laplace Distribution and Gen-*

- eralizations: A revisit with applications to communications, economics, engineering and finance.* Birkhauser, Boston, USA. pp. 133-144.
- [28] Reed, W. (2006). The Normal-Laplace distribution and its relatives. In: Balakrishnan, N., Castillo, E., Sarabia Alegria, J.-M. (eds.) *Advances in Distribution Theory, Order Statistics, and Inference*, pp. 61–74. Birkhäuser Boston, New York.
  - [29] Amini Z; & Rabbani, H. (2017). Letter to the editor: Correction to “The Normal-Laplace distribution and its relatives”, *Communications in Statistics - Theory & Methods*, 46(4), 2076-2078.
  - [30] Evans, M.J & Rosenthal, J.S. (2010). *Probability and Statistics: The Science of Uncertainty* (2ed). W. H. Freeman and Company: New York, USA. p. 167.
  - [31] Luce, R.D. (1986). *Response Times: Their Role in Inferring Elementary Mental Organizations* (No.8). Oxford University Press: New York, USA. 16,24
  - [32] Signorell A; Aho K; Alfons A; Anderegg N; Aragon T; Arachchige C; et al. (2020). *DescTools: Tools for Descriptive Statistics*. R package version 0.99.38, <https://cran.r-project.org/package=DescTools>.
  - [33] Reed, W.J. & Jorgensen, M. (2004). The Double Pareto-lognormal distribution-A New Parametric Model for Size Distributions. *Communications in Statistics-Theory & Methods*, 33: 1733-1753.



## Appendices

### Appendix A. Proofs

This appendix presents proofs for the new results presented in Section 3.1.

#### A.1. Proof of Theorem 3.1.

**Proof.** Let  $\Delta GORT = GORT_B - GORT_A$  where  $GORT_B, GORT_A$  are independent with ExG distribution with associated parameters  $\theta_B = (\mu_B, \sigma_B, \tau_B), \theta_A = (\mu_A, \sigma_A, \tau_A)$ , respectively. Then, by Definition.2.1, Definition.2.2 and Theorem.2.4 it follows that:

$$\begin{aligned}
 m_{\Delta GORT}(t) &= m_{GORT_B}(t) \times m_{GORT_A}(-t) \\
 &= m_{ExG(\theta_B)}(t) \times m_{ExG(\theta_A)}(-t) \\
 &= ((1 - t\tau_B)^{-1} \exp(\mu_B.t + \frac{\sigma_B^2}{2}t^2)) \times ((1 + t\tau_A)^{-1} \exp(-\mu_A.t + \frac{\sigma_A^2}{2}t^2)) \\
 &= ((1 - t\tau_B)(1 + t\tau_A))^{-1} \exp((\mu_B - \mu_A).t + \frac{\sigma_B^2 + \sigma_A^2}{2}t^2) \\
 &= (1 + (\tau_A - \tau_B)t - \tau_A\tau_B.t^2)^{-1} \exp((\mu_B - \mu_A).t + \frac{\sigma_B^2 + \sigma_A^2}{2}t^2) \\
 &= m_{AL(\tau_A, \tau_B)}(t) \times m_{N(\mu_B - \mu_A, \sigma_B^2 + \sigma_A^2)}(t) : -\tau_A^{-1} < t < \tau_B^{-1}.
 \end{aligned}$$

Accordingly, by Theorem2.5 it follows that:

$$\Delta GORT =^d AL(\tau_A, \tau_B) \oplus N(\mu_B - \mu_A, \sigma_B^2 + \sigma_A^2).$$

□

#### A.2. Proof of Theorem 3.2.

**Proof.** By Definition2.2 and Theorem2.4 for the nth cumulant of the ALG distribution with four parameters  $(\alpha_1, \alpha_2, \mu, \sigma)$  we have:

$$\begin{aligned}
 \kappa_n^{ALG(\alpha_1, \alpha_2, \mu, \sigma)} &= \kappa_n^{AL(\alpha_1, \alpha_2)} + \kappa_n^{N(\mu, \sigma^2)} \\
 &= ((n-1)!((- \alpha_1)^n + \alpha_2^n)) + (1_{(n=1)}(n)\mu + 1_{(n=2)}(n)\sigma^2) : 1 \leq n.
 \end{aligned}$$

Consequently, the descriptive and the shape statistics for the ALG distribution with four parameters  $(\alpha_1, \alpha_2, \mu, \sigma)$ , it follows that:

$$\begin{aligned}
 \text{Mean} & E(ALG) = \alpha_2 - \alpha_1 + \mu, \\
 \text{Variance} & Var(ALG) = \alpha_1^2 + \alpha_2^2 + \sigma^2, \\
 \text{Skewness} & \gamma_{ALG} = \frac{2(\alpha_2^3 - \alpha_1^3)}{(\alpha_1^2 + \alpha_2^2 + \sigma^2)^{3/2}}, \\
 \text{Kurtosis} & \kappa_{ALG} = \frac{6(\alpha_1^4 + \alpha_2^4)}{(\alpha_1^2 + \alpha_2^2 + \sigma^2)^2}.
 \end{aligned}$$

Finally, the assertion follows for  $\alpha_1 = \tau_A, \alpha_2 = \tau_B, \mu = \mu_B - \mu_A$ , and  $\sigma^2 = \sigma_B^2 + \sigma_A^2$ .

□

### A.3. Proof of Theorem 3.3.

**Proof.** Given a four parametric  $ALG(\alpha_1, \alpha_2, \mu, \sigma)$  for the proactive inhibition. Then, it can be written in the form:

$$ALG(\alpha_1, \alpha_2, \mu, \sigma) = \mu \oplus \sigma N(0, 1) \oplus \alpha_2 Exp_2(1) \oplus \alpha_1 Exp_1(1)$$

where the random variables  $N(0, 1), Exp_i(1) \sim Exp(1) (i = 1, 2)$  are mutually independent. Accordingly, there are uncountably many solutions  $(\mu_A, \sigma_A, \tau_A, \mu_B, \sigma_B, \tau_B)$  for the following equations:

$$\tau_A = \alpha_1, \tau_B = \alpha_2, \mu_B - \mu_A = \mu, \sigma_B^2 + \sigma_A^2 = \sigma^2.$$

□

### A.4. Proof of Theorem 3.4.

**Proof.** These are straightforward from the probability density function and [28].

□

### A.5. Proof of Theorem 3.5.

**Proof.** Let,  $\Delta GORT \stackrel{d}{=} ALG(\alpha_1, \alpha_2, \mu, \sigma) \stackrel{d}{=} AL(\alpha_1, \alpha_2) \oplus N(\mu, \sigma^2)$  where  $(\alpha_1, \alpha_2, \mu, \sigma^2) = (\tau_A, \tau_B, \mu_B - \mu_A, \sigma_A^2 + \sigma_B^2)$ . For,  $X \stackrel{d}{=} AL(\alpha_1, \alpha_2), Y \stackrel{d}{=} N(\mu, \sigma^2)$ , and two applications of Theorem 2.6 for the following convex functions show that both components of the ALG distribution have increasing hazard functions:

$$\begin{aligned} -\ln(f_X(t)) &= \ln(\alpha_1 + \alpha_2) \times \left( \frac{-t}{\alpha_1} 1_{(-\infty, 0]} + \frac{t}{\alpha_2} 1_{[0, \infty)}(t) \right) \quad -\infty < t < \infty, \\ -\ln(f_Y(t)) &= \ln(\sqrt{2\pi}\sigma) + \frac{(t - \mu)^2}{2\sigma^2}. \quad -\infty < t < \infty \end{aligned}$$

Accordingly, by an application of the Theorem 2.7, the plausible result follows.

□

## Appendix B. ExG models parameters

This appendix presents IBPA parameter estimations for cluster type ExG model.

**Table B1.:** Mean posterior Ex-Gaussian parameters estimations across trial types by IBPA ( $n = 44$ ).

#	$\mu$ - parameter			$\sigma$ - parameter			$\tau$ - parameter		
	$\mu_S$	$\mu_A$	$\mu_B$	$\sigma_S$	$\sigma_A$	$\sigma_B$	$\tau_S$	$\tau_A$	$\tau_B$
1	357	350	372	32	35	14	86	96	68
2	637	599	732	175	170	132	47	48	68
3	469	484	411	60	57	42	76	73	111
4	597	567	631	163	165	96	66	69	149
5	640	618	608	156	133	58	47	62	121
6	452	431	469	108	106	64	66	65	135
7	689	668	664	136	130	146	47	60	115
8	665	609	660	145	91	237	51	103	120
9	543	484	640	166	151	118	120	147	157
10	470	468	483	56	59	52	98	87	156
11	414	399	597	46	37	118	177	168	80
12	557	534	597	132	128	146	53	58	123
13	550	538	564	137	133	98	55	38	190
14	319	318	365	307	295	370	170	137	264
15	421	416	437	61	56	90	138	142	149
16	358	342	389	61	57	61	48	56	57
17	594	599	561	130	130	133	78	62	196
18	467	397	747	229	190	299	127	131	159
19	426	426	424	67	75	50	102	103	110
20	423	449	504	62	74	129	122	65	169
21	521	519	487	144	157	96	91	97	125
22	397	346	463	87	58	110	94	132	101
23	540	525	588	80	78	79	94	88	128
24	592	571	529	176	136	304	46	69	180
25	577	459	602	165	70	244	69	181	124
26	562	555	694	79	75	160	172	154	148
27	446	436	541	71	60	166	240	236	233
28	486	476	629	82	64	196	172	155	151
29	414	363	391	133	66	213	62	115	111
30	486	484	541	87	86	146	141	127	181
31	546	502	656	137	118	157	90	100	137
32	436	421	462	107	109	90	72	81	88
33	452	454	458	38	46	40	156	156	165
34	404	422	408	105	109	42	95	72	92
35	470	549	595	230	200	298	207	171	136
36	429	400	448	116	139	95	158	163	245
37	521	497	507	89	130	68	112	125	222
38	284	271	321	40	37	53	100	108	91
39	424	432	416	57	55	87	70	52	131
40	419	418	476	52	53	196	145	148	105
41	533	537	517	105	151	93	72	35	159
42	388	445	497	53	145	206	145	57	116
43	506	467	539	97	82	100	66	96	78
44	842	824	822	175	341	165	34	95	320

Notes:  $\mu_S, \sigma_S, \tau_S$  : ExG GORT parameters for single cluster SST data;  $\mu_A, \sigma_A, \tau_A$  : ExG GORT parameters for type-A cluster SST data;  $\mu_B, \sigma_B, \tau_B$  : ExG GORT parameters for type-B cluster SST data; IBPA: #Chains = 3; Simulations = 20,000; Burn-in<sub>0</sub> = 5,000 (for all parameters).